The impact of particle size and volatile organics on the light absorption of wildfire-like brown carbon emissions from wood combustion

Moularas, Constantinos; Tsiodra, Irini; Mihalopoulos, Nikolaos; Demokritou, Philip; Kelesidis, Georgios A.

DOI
10.1016/j.envint.2025.109626

Publication date
2025

Document Version
Final published version

Published in
Environment International

Citation (APA)
Moularas, C., Tsiodra, I., Mihalopoulos, N., Demokritou, P., & Kelesidis, G. A. (2025). The impact of particle size and volatile organics on the light absorption of wildfire-like brown carbon emissions from wood combustion. *Environment International*, *202*, Article 109626. https://doi.org/10.1016/j.envint.2025.109626

Environment International 202 (2025) 109626

Contents lists available at ScienceDirect

Environment International

journal homepage: www.elsevier.com/locate/envint

Full length article

The impact of particle size and volatile organics on the light absorption of wildfire-like brown carbon emissions from wood combustion

Constantinos Moularas [a,b], Irini Tsiodra [c], Nikolaos Mihalopoulos [c,d], Philip Demokritou [a], Georgios A. Kelesidis [a,b,*]

[a] Nanoscience and Advanced Material Center, Environmental and Occupation Health Science Institute, School of Public Health, Rutgers University, Frelinghuysen 170, 08854 Piscataway, NJ, USA
[b] Faculty of Aerospace Engineering, Delft University of Technology, Delft 2629 HS, the Netherlands
[c] Institute for Environmental Research and Sustainable Development, National Observatory of Athens, Lofos Koufou, Palea Penteli, Athens 15236, Greece
[d] Environmental Chemical Processes Laboratory, Department of Chemistry, University of Crete, Heraklion 71003, Greece

ARTICLE INFO

Editor: Xavier Querol

Keywords:
Wildfires
Wood combustion
Brown carbon
Light absorption
PAHs

ABSTRACT

Here, the light absorption of brown carbon (BrC) emitted by wood combustion and denuded from volatile organic carbon (VOC) at 300 °C is elucidated using a recently developed thermal decomposition platform coupled with a suite of real-time aerosol instrumentation and time-integrated sampling systems. The BrC particle size distribution, morphology and optical properties are closely controlled by increasing the combusted wood mass from 50 to 600 mg to emulate those measured for "real world" wildfire particulate matter (PM) emissions. Size-fractionation of such wildfire-like BrC reveals that the $PM_{0.1–2.5}$ fraction contains high molecular weight, carcinogenic polycyclic aromatic hydrocarbons (PAHs) and absorbs up to five times more light compared to the $PM_{0.1}$ fraction. Thus, increasing the combusted wood mass from 50 to 600 mg increases the $PM_{0.1–2.5}$ concentration by a factor of about eight and enhances the overall BrC mass absorption cross-section, *MAC*, up to a factor of two at a wavelength of 405 nm. Condensation of VOC on BrC reduces its *MAC* up to 40 %. Still, the particle size seems to largely determine the BrC light absorption, as large VOC-rich particles absorb more light compared to small VOC-lean ones. The size-resolved BrC *MAC* measured here can be interfaced with climate models to estimate the climate impact of wildfire PM emissions.

1. Introduction

The frequency and intensity of wildfires has increased substantially due to climate change (Jones et al., 2022). Extreme wildfire incidents in Western US (Liu et al., 2016), Canada (Kirchmeier-Young et al., 2019) or the Mediterranean region (Kaskaoutis et al., 2024) result in large concentrations of particulate matter (PM) emissions that can be transported over long distances, reach metropolitan areas (e.g. New York City (Laurent et al., 2024)) and affect millions of people.

The exposure to PM emissions from wildfires is linked to respiratory (Larson and Koenig, 1994), cardiovascular (Khraishah et al., 2022) and neurological (Schuller and Montrose, 2020) disorders. At the same time, wildfire PM emissions can cool (Zhang et al., 2017; Kelesidis et al., 2025) or warm (Chakrabarty et al., 2023) the climate depending on their physicochemical properties and change the wildfire dynamics (Yu et al., 2019; Wang et al., 2024). So, a detailed characterization of wildfire PM emissions in terms of size-fractionation and chemical composition is essential to quantify and mitigate their impact on public health and climate change.

The PM emissions from wildfires contain mostly (≥80 wt%) organic carbon (OC) aerosols, as well as small concentrations (<20 wt%) of black or elemental carbon (EC) (Chakrabarty et al., 2023; China et al., 2013; Li et al., 2024). Brown carbon (BrC) is often considered a subset of volatile OC (VOC) (Laskin et al., 2015). Here, BrC refers to the refractory, light absorbing component of OC that is not vaporized after thermal denuding at 300 °C (Moularas et al., 2024). Mobility (Wardoyo et al., 2007) and microscopy image (Chakrabarty et al., 2023; China et al., 2013) analysis revealed that BrC particles are rather spherical and have a mean diameter ranging from 43 to 270 nm (Chakrabarty et al., 2006). Laboratory (Samburova et al., 2016) and field (Laurent et al., 2024; Vicente et al., 2012; Wentworth et al., 2018; Verma et al., 2007) studies have shown that BrC particles emitted by biomass combustion

* Corresponding author.
E-mail address: g.kelesidis@tudelft.nl (G.A. Kelesidis).

https://doi.org/10.1016/j.envint.2025.109626
Received 7 March 2025; Received in revised form 21 May 2025; Accepted 20 June 2025
Available online 21 June 2025

during wildfires contain retene, as well as some of the 16 polycyclic aromatic hydrocarbons (PAHs) that have been prioritized by the Environmental Protection Agency (EPA). This has raised concerns regarding the public health impact of BrC, given the recent wildfire events in the US and elsewhere with extremely high concentrations of wildfire PM impacting even major metropolitan areas, such as New York City (Laurent et al., 2024) and Los Angeles (Künzli et al., 2003).

The climate effect of wildfire PM emissions is determined by their light absorption that is quantified by the mass absorption cross-section, *MAC* (Olson et al., 2015), and ranges from $0.4 - 0.75\ m^2/g$ (Carter et al., 2021; Zeng et al., 2022; Kleinman et al., 2020; Washenfelder et al., 2022; Bali et al., 2024; Marsavin et al., 2021). In this regard, the link between the BrC *MAC* and its physicochemical properties has been explored to reduce the uncertainty regarding the climate impact from wildfire PM emissions. For instance, laboratory (Saleh et al., 2014) and field (Shetty et al., 2023) studies indicated that the light absorption of BrC particles increases with decreasing volatility. So, PAHs with relatively low molecular weight (such as retene) account for just 0.03–0.16 % of the total BrC light absorption (Samburova et al., 2016). Size exclusion chromatography coupled with UV–vis spectroscopy showed that high molecular weight organic species with extremely low volatility (Di Lorenzo et al., 2017) are the main contributors to the BrC light absorption (Di Lorenzo and Young, 2016). The light absorption of these species is affected less by photochemical ageing compared to species having lower molecular weights (Di Lorenzo et al., 2017; Wong et al., 2017). Most importantly, size-resolved measurements of the BrC composition showed that the concentration of the high molecular weight compounds increases with increasing particle size (Di Lorenzo et al., 2018).

The above findings highlight the need for climate models to account for the variation of the BrC light absorption with the particle volatility and size (Saleh, 2020). To this end, Saleh et al. (Saleh et al., 2014) related the imaginary part of the BrC refractive index to the ratio of black carbon or EC over the organic aerosol to account indirectly for the variation of the particle volatility. However, this relation resulted in a large overestimation of the BrC *MAC* measured in wildfires (Shen et al., 2024). This indicates that new parametrizations are needed for the BrC light absorption to account for both the particle size and composition. Even though the light absorption of PAHs extracted from BrC particles has been measured extensively (Shetty et al., 2023; Di Lorenzo et al., 2017; Di Lorenzo and Young, 2016; Wong et al., 2017; Di Lorenzo et al., 2018), the *MAC* of size-fractionated BrC particles has not been characterized yet, to the best of our knowledge.

In this regard, a recently developed by the authors thermal decomposition platform (called integrated exposure generation system, INEXS) has been coupled with a variety of real-time monitoring and time-integrated sampling instrumentation (Moularas et al., 2024; Singh et al., 2022; Singh et al., 2023) to elucidate the BrC dynamics during wood combustion. That way, the BrC aerodynamic, mobility size and mass distributions, surface chemistry (Singh et al., 2022; Singh et al., 2023) and light absorption (Moularas et al., 2024) have been measured in real time for PM emissions from combustion of various wood types at well controlled temperature and O_2 conditions. Here, INEXS is used to quantify the impact of particle size and VOC on the light absorption dynamics of BrC emitted by combustion of the following wood types: i) pine, a characteristic softwood containing mostly retene; and ii) oak, a hardwood containing several high molecular weight PAH species. The particle size distribution, morphology and optical properties are closely controlled by varying the combusted wood mass to generate wildfire-like BrC. The VOC content of the BrC particles produced here is also varied by thermal denuding at 0–300 °C. Most importantly, the *MAC* of size-fractionated BrC particles with and without VOC is obtained to elucidate the effect of the coating and particle size on the BrC light absorption, for the first time to the best of our knowledge.

2. Materials & methods

The dynamics of BrC particles during wood combustion are investigated using the INEXS platform (Fig. 1) that has been described in detail previously (Moularas et al., 2024; Singh et al., 2022; 2023). The combustion conditions used in the INEXS platform are varied to produce BrC particles that are representative of wildfire PM. In brief, 50–600 mg of pine and 600 mg of oak wood powder are produced by grinding commercial wood pellets (Pine Mountain Starter Stikk Fatwood, Royal Oak Enterprises LLC, Roswell, GA; oak wood procured from Home Depot) and placed into a high-purity quartz crucible at the middle of a quartz tube furnace (length: 100 cm; inner diameter: 5 cm) (Moularas et al., 2024; Singh et al., 2022; 2023). Above the crucible, synthetic air (80 vol % N_2, 20 vol% O_2) flows at 6 L/min. The furnace T is increased at a rate of 40 °C/min reaching a maximum temperature of 800 °C at about 22 min. The temperature is held at 800 °C for another 8 min before the combustion of wood has been completed and the reactor is cooled to room temperature. Since the atmosphere in the tube furnace contains 20 vol% O_2, the dominant process is combustion rather than pyrolysis. Detailed monitoring of the transition from smoldering to flaming wood combustion conditions in tube reactors (Garg et al., 2023) indicate that mostly smoldering combustion takes place when air flows at rather small velocities (5 cm/s) above wood powder with rather low densities (~1.5 g/cm^3 (Moularas et al., 2024)), such as those used here. Also, no flame was observed visually at any of the conditions investigated here, further confirming that smoldering wood combustion conditions are present.

The aerosol emissions exiting INEXS are directed to a real-time particle monitoring and time-integrated PM sampling instrumentation (Moularas et al., 2024; Singh et al., 2022; 2023). Most wildfire PM (~90 %) contains semi- and non-volatile BrC particles (Zheng et al., 2020). So, the BrC particles generated here are thermally denuded at 300 °C to facilitate consistent comparisons to field measurements of wildfire PM. In particular, BrC particles are denuded from condensed volatile organic carbon (VOC) aerosols using a thermal denuder (Dekati Thermodenuder, Finland) that is pre-heated at a temperature, T_d = 300 °C. Thermal denuding at T_d = 300 °C is commonly used to quantify the BrC light absorption in the absence of condensed organics (Saleh et al., 2018). In addition, T_d is reduced from 300 to 0 °C to elucidate the impact of VOC on the light absorption of BrC. The mass concentration of the non-denuded BrC is practically identical with that obtained for BrC denuded at T_d = 100 °C (see section 3.3), indicating that evaporation does not affect the non-denuded samples. The emitted BrC particle size distribution is monitored every 2 mins using a Scanning Mobility Particle Sizer (SMPS, model 3080, TSI) to obtain the total number concentration of particles with mobility diameter ranging from 5 to 200 nm (Fig. S1). Due to the high emitted particle concentrations, a rotating disk thermodiluter (model 379020A, TSI) is used before SMPS to dilute the aerosol by a factor of 500. The BrC mobility size distribution obtained at the peak number concentration is reported (Fig. S2). Note that SMPS measurements were performed to compare the number-based mobility size distribution of the generated BrC to those measured for wildfire PM.

The emitted aerosols are also fractionated into $PM_{0.1}$, $PM_{0.1–2.5}$, $PM_{2.5–10}$, and $PM_{>10}$ aerodynamic size fractions using a Compact Cascade Impactor (CCI) (Demokritou et al., 2004; Sotiriou et al., 2015) developed by the authors. The cutoff diameters are given in μm. The $PM_{2.5}$ size fraction can be also selected by removing the $PM_{0.1}$ stage. So, the $PM_{0.1}$ and $PM_{2.5}$ fractions are directed to a photoacoustic extinctionmeter (PAX, Droplet Measurement Technologies), where the absorption coefficient, b_{abs}, at 405 nm is monitored every 1 s (Fig. S3 & S4). Since BrC absorbs mostly UV–visible light, a wavelength of 405 nm is appropriate for the *MAC* calculation and has been already used both in field (Carter et al., 2021) and laboratory (Shen et al., 2024) studies. The light absorbing $PM_{0.1}$ and $PM_{2.5}$ having $b_{abs} > 0\ Mm^{-1}$ are collected on Teflon filters (PTFE membrane disc filter: 2 μm pore size, 47 mm diameter, Pall Corporation, Port Washington, NY), as described previously (Demokritou et al., 2004; Sotiriou et al., 2015). Lacey carbon

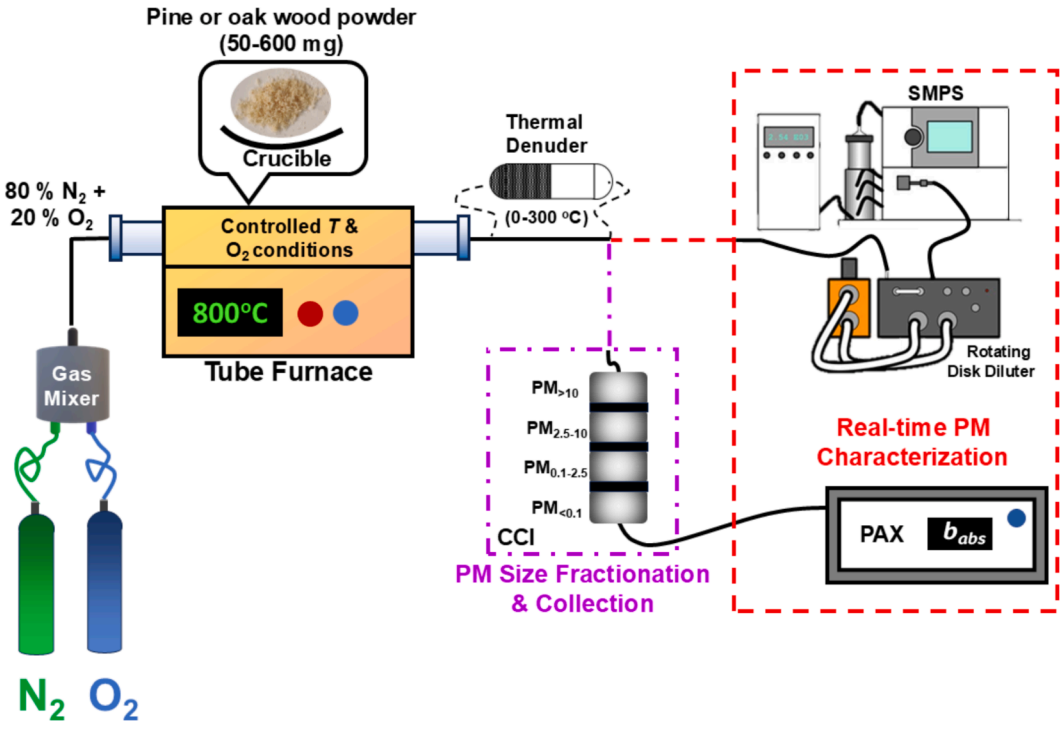

Fig. 1. Schematic of the integrated and exposure generation system (INEXS) used for combustion of pine and oak wood powder. The INEXS platform is connected to a variety of real-time monitoring and time-integrated sampling instrumentation, including a thermal denuder for removal of VOC, a scanning mobility particle sizer (SMPS), a cascade compact impactor (CCI) for size fractionation and collection of particulate matter and a photoacoustic photoacoustic extinctionmeter (PAX).

transmission electron microscopy grids with a 200 mesh copper support (LC200-Cu-150, Electron Microscopy Sciences) were placed in the middle of the Teflon filter to collect particles from the $PM_{2.5}$ fraction. Gravimetric analysis of the collected $PM_{0.1}$ and $PM_{2.5}$ (without the presence of microscopy grids) is done using an analytical microbalance (Mettler Toledo, Columbus, OH) to calculate the average mass concentrations $M_{PM0.1}$ and $M_{PM2.5}$ of the light absorbing particles in the $PM_{0.1}$ and $PM_{2.5}$ fractions, respectively. The average absorption coefficients, $<b_{abs}>$, for the different PM cutoff sizes, are measured sequentially in two separate runs. To quantify the uncertainty, three independent b_{abs} measurements were done resulting in a relative error of about 13 %. Each measurement was repeated three times for each wood mass. The average $MAC_{PM0.1}$ and $MAC_{PM2.5}$ are obtained using the time-averaged $< b_{abs,PM0.1} >$ and $M_{PM0.1}$ of the $PM_{0.1}$ fraction (Islam et al., 2022):

$$MAC_{PM0.1} =< b_{abs,PM0.1} > /M_{PM0.1} \quad (1)$$

and the $< b_{abs,PM2.5} >$ and $M_{PM2.5}$ of the $PM_{2.5}$ fraction (Islam et al., 2022):

$$MAC_{PM2.5} =< b_{abs,PM2.5} > /M_{PM2.5} \quad (2)$$

The mass concentration, $M_{PM0.1–2.5}$, of the $PM_{0.1–2.5}$ fraction is given by:

$$M_{PM0.1-2.5} = M_{PM2.5} - M_{PM0.1} \quad (3)$$

and, similarly, its $< b_{abs,PM0.1-2.5} >$ by:

$$< b_{abs,PM0.1-2.5} >=< b_{abs,PM2.5} > - < b_{abs,PM0.1} > \quad (4)$$

Based on Eqs. (1), (2) and (4), the $MAC_{PM0.1–2.5}$ is obtained by:

$$MAC_{PM0.1-2.5} = (M_{PM2.5}MAC_{PM2.5} - M_{PM0.1}MAC_{PM0.1})/M_{PM0.1-2.5} \quad (5)$$

It should be noted that the BrC *MAC* estimated by integrating the b_{abs} curve over time results in identical *MAC* values with those obtained using Eqs. (1) and (2). The time-averaged *MAC* is about 20 % larger than the instantaneous one due to variations of the BrC physicochemical properties during wood combustion (Fig. S5). The light absorption of BrC spheres with a diameter of 10–2500 nm and bulk density of 1.3 g/cm^3 was derived based on the Mie theory (Kelesidis et al., 2024) using Maetzler's MATLAB code (Maetzler, 2002). A BrC refractive index, $RI = 1.55–0.017i$ was used as it has described accurately the *MAC* of wildfire BrC at a wavelength of 405 nm (Kelesidis et al., 2025). The imaginary part of the *RI* is also reduced by 65 % to elucidate the optical properties of BrC containing VOC and other PAHs with small light absorption efficiency.

The PAHs adsorbed on the sampled $PM_{0.1}$ and $PM_{2.5}$ size fraction were obtained using the protocol described in Tsiodra et al. (Tsiodra et al., 2021) with slight modifications given in Laurent et al. (Laurent et al., 2024). The analysis focused on the identification of 25 PAHs with molecular weight between 178 to 302 g/mol. The analysis of elemental and organic carbon (EC-OC) was done for the $PM_{2.5}$ size fraction using the thermal-optical transmission (TOT) technique with a Sunset carbon analyzer (Sunset Laboratory Inc., Portland, OR, USA) and the EUSAAR2 thermal protocol described in detail by Cavalli et al. (Cavalli et al., 2010). The microscopy grids containing the $PM_{2.5}$ fraction of BrC were imaged using transmission electron microscopy (TEM, JEOL-2010F).

3. Results & discussion

3.1. Generation and characterization of wildfire-like BrC $PM_{2.5}$ emissions

Combustion of various wood types (pine and oak) and masses (50–600 mg) is explored in this section to generate BrC particles with controlled size distribution, morphology and optical properties that emulate those measured for wildfire PM. For example, microscopy analysis of $PM_{2.5}$ emitted by combustion of 50 (Fig. 2a), 100 (b), 300 (c) and 600 mg (d) of pine wood reveal that spherical BrC particles are produced regardless of the combusted wood mass. Similar spherical BrC particles have been identified in PM emissions from wildfires in New Mexico (China et al., 2013) (e) and Western US (Chakrabarty et al., 2023) (f). Smoldering combustion conditions were present during

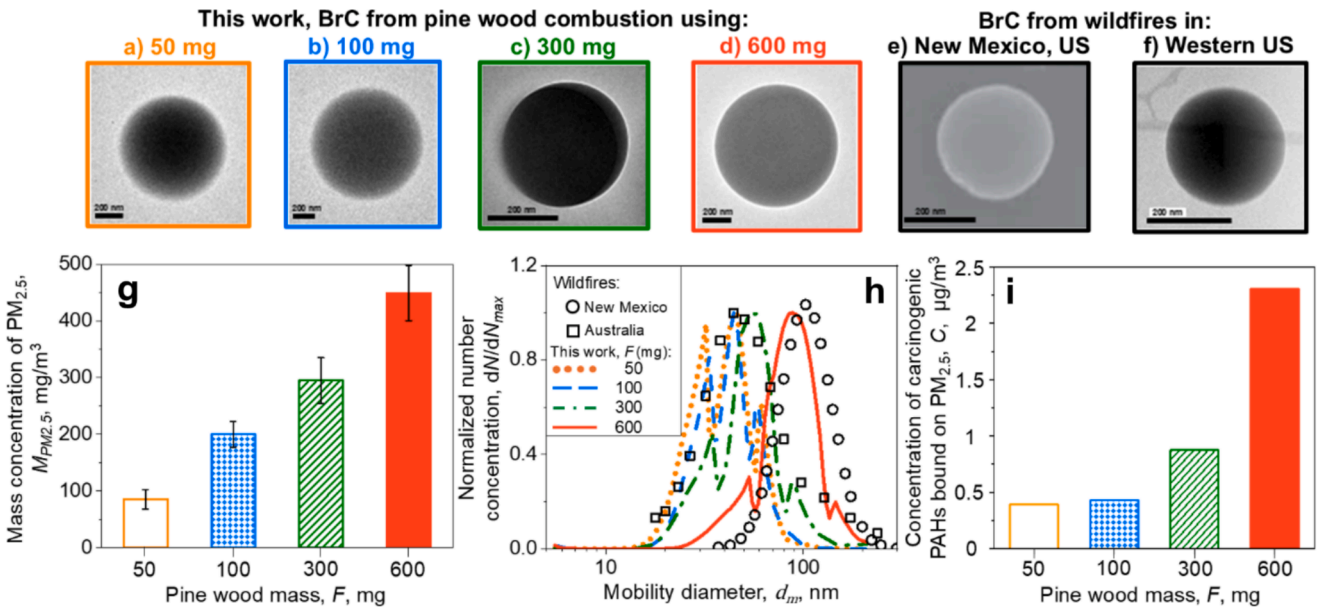

Fig. 2. Physicochemical characterization of Brown Carbon (BrC) particles from wood combustion and comparison to wildfire PM emissions. (a–f) Microscopy images of BrC particles emitted by combustion of 50 (a), 100 (b), 300 (c) and 600 mg (d) of pine wood with air compared to those measured from wildfire emissions in New Mexico (China et al., 2013) (e) and Western US (Chakrabarty et al., 2023) (f). (g-i) Mass concentration, $M_{PM2.5}$ (g), mobility size distribution (h) and carcinogenic PAH concentration, C (i), measured for the $PM_{2.5}$ fraction of BrC emitted by combustion of 50 (orange open bars & dotted line), 100 (blue dotted bars & broken line), 300 (green lined bars & dot-broken line) and 600 mg (red filled bar & solid line) of pine wood. The BrC mobility size distributions measured here are compared to those measured from fresh wildfire PM in Australia (squares (Wardoyo et al., 2007)) and New Mexico, US (circles (China et al., 2013)). (For interpretation of the references to colour in this figure legend, the reader is referred to the web version of this article.)

sampling of BrC particles from the New Mexico wildfire (China et al., 2013) that are similar to those present in the INEXS platform. The spherical BrC particles measured in this work are very similar to the so-called tar balls identified in wildfire PM (Chakrabarty et al., 2010; Corbin et al., 2019). These tar balls are often associated with strong light absorption (Chakrabarty et al., 2023). The light absorption of single BrC particles could not be measured with the available instrumentation and, thus, the presence of strongly absorbing tar balls could not be verified.

Combustion of 50 mg of pine wood results in $PM_{2.5}$ mass concentration of 80 ± 17 mg/m^3 emissions (Fig. 2g: orange open bar). The number-based mobility size distribution of these emissions is multi-modal, having a mean mobility diameter of about 41 nm (Fig. 2h: dotted line & Fig. S2a). Multi-modal size distributions are typically obtained when nucleation generates continuously new small particles, while existing particles grow larger by coagulation and surface reactions or condensation (Abid et al., 2008). This creates distinct peaks in the BrC size distribution. The mobility size distribution obtained here by combustion of 50 mg of pine wood is less smooth compared to that obtained previously using the same set up and pine wood mass (Moularas et al., 2024). This can be attributed to the larger combustion temperature (800 °C vs 400 °C) and heating rate (40 °C/min vs 20 °C/min) used here. Increasing the pine wood mass from 50 to 600 mg increases the PM mass concentration by a factor of five (Fig. 2g: red filled bar). The large $PM_{2.5}$ mass concentration obtained by combustion of 600 mg of pine wood enhances the particle coagulation resulting in large BrC particles having a mean diameter of 87 nm (Fig. 2h: solid line). The increase of the BrC mass concentration and mean mobility diameter can be attributed to the enhancement of the equivalence ratio with increasing pine wood mass. Similar trends have been reported for soot nanoparticles produced in premixed ethylene flames at increasing equivalence ratios (Maricq et al., 2003). Similar variations of the BrC mobility size distribution with the wildfire intensity (Wardoyo et al., 2007) and oxygen content (China et al., 2013) have been observed in field measurements. Combustion of 600 mg of oak wood results in similar mass concentration with that obtained for pine wood (~450 ± 49 mg/m^3) and slightly larger BrC particles with mean diameter of about 99 nm (Fig. S6). The mobility size distribution of BrC can be controlled well by varying the wood mass and type and reproduce the size distributions measured for wildfire PM emissions. For instance, the mobility size distributions measured for BrC generated by combustion of 300 (Fig. 2h: dot-broken line) and 600 mg (solid line) are in good agreement with those measured for emissions from wildfires in Australia (Wardoyo et al., 2007) (squares) and New Mexico, US (China et al., 2013) (circles), respectively.

Fig. 2i shows the concentration, C, of the carcinogenic PAHs bound on $PM_{2.5}$ generated by combustion of 50 (orange open bar), 100 (blue dotted bar), 300 (green lined bar) and 600 mg (red filled bar) of pine wood. It should be noted that the $PM_{2.5}$ presented in Fig. 2i has been thermally denuded at 300 °C to remove most of the adsorbed volatile organic species (see discussion in section 3.3). The concentration shown in Fig. 2i has been obtained by summing up the concentration of PAHs found in the classification groups 1, 2a and 2b of the Internation Agency for Research on Cancer. The concentration of these carcinogenic PAHs is increasing with increasing pine wood mass. Such PAH species have been measured previously in $PM_{2.5}$ emissions from forest fires in Greece (Tsiodra et al., 2024), Portugal (Vicente et al., 2012), western US (Verma et al., October 2007) and Canada (Wentworth et al., 2018) transported to Northeast US (Laurent et al., 2024). In addition to the carcinogenic PAHs shown in Fig. 2i, large concentrations of retene were measured also on the $PM_{2.5}$ sampled from combustion of 50–600 mg of pine wood (Fig. S7). This is expected, as retene is a standard molecular marker of wood combustion (Ramdahl, 1983) and has been measured previously in wildfire smoke (Laurent et al., 2024; Vicente et al., 2012; Wentworth et al., 2018). Combustion of oak wood results in BrC particles containing similar concentrations of retene compared to those measured for BrC from pine wood combustion, but larger concentrations of carcinogenic PAHs (Fig. S8). In addition to these PAHs, BrC particles emitted by oak wood combustion contain large concentrations of oxygenated PAHs (Fig. S8).

Fig. 3a shows the mass absorption cross-section, $MAC_{PM2.5}$, measured at 405 nm for the $PM_{2.5}$ fraction of BrC emitted by combustion of 50 (orange open bar), 100 (blue dotted bar), 300 (green lined bar) and 600 mg (red filled bar) of pine wood. During combustion of 50 mg of

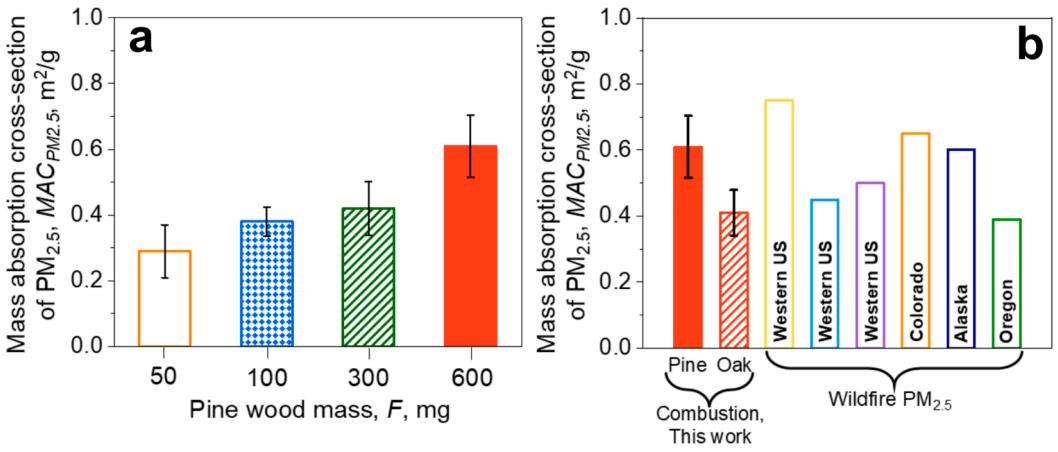

Fig. 3. Impact of wood mass and type on BrC light absorption. (a) Mass absorption cross-section, $MAC_{PM2.5}$, of the $PM_{2.5}$ fraction of BrC emitted by combustion of 50 (orange open bar), 100 (blue dotted bar), 300 (green lined bar) and 600 mg (red filled bar) of pine wood measured at 405 nm. (b) The $MAC_{PM2.5}$ measured for the $PM_{2.5}$ emissions from combustion of 600 mg of pine (red filled bar) and oak (red lined bar) compared to those measured from wildfire $PM_{2.5}$ emissions (open bars (Carter et al., 2021; Zeng et al., 2022; Kleinman et al., 2020; Washenfelder et al., 2022; Bali et al., 2024; Marsavin et al., 2021)). (For interpretation of the references to colour in this figure legend, the reader is referred to the web version of this article.)

pine wood at 800 °C, BrC particles with $MAC_{PM2.5} = 0.3 \pm 0.08$ m^2/g are emitted, consistent with the $MAC_{PM2.5}$ of 0.27 m^2/g obtained for BrC from pine wood combustion at 400 °C (Moularas et al., 2024). Increasing the fuel mass from 50 to 600 mg increases the BrC $MAC_{PM2.5}$ to 0.6 ± 0.09 m^2/g. Combustion of 600 mg of oak wood generates BrC particles with $MAC_{PM2.5}$ = 0.4 ± 0.07 m^2/g (Fig. 3b: red lined bar). The $MAC_{PM2.5}$ = 0.3–0.6 m^2/g measured here at 405 nm for BrC particles from pine and oak wood combustion is in good agreement with the *MAC* measured for emissions from wildfires in western US (Fig. 3b: yellow (Carter et al., 2021), light blue (Zeng et al., 2022) and purple (Kleinman

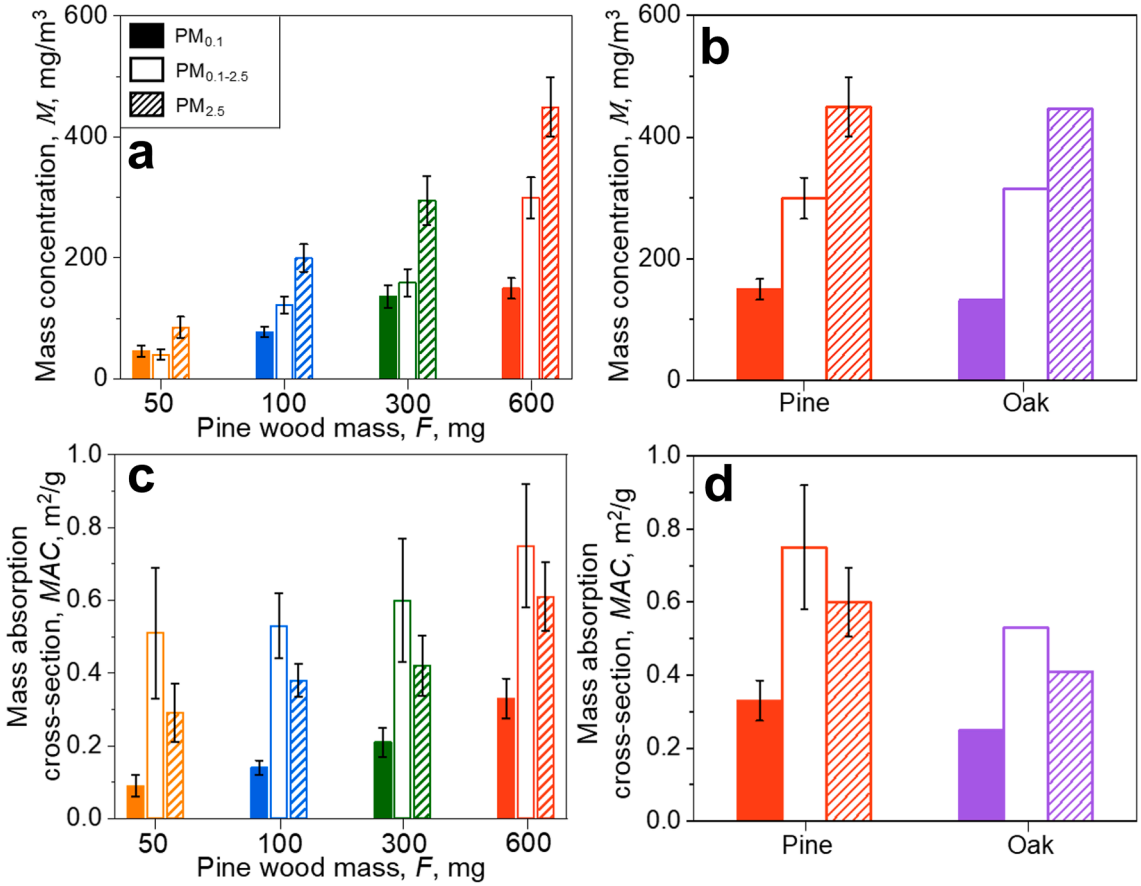

Fig. 4. Mass concentration and light absorption of size-fractionated BrC partcles. (a, b) Mass concentration, *M*, of the $PM_{0.1}$ (solid bars), $PM_{0.1–2.5}$ (open bars) and $PM_{2.5}$ (lined bars) fractions of BrC emitted by combustion of 50 (orange bars), 100 (blue bars), 300 (green bars) and 600 mg (red bars) of pine (a) and oak (b: purple bars) wood. (c, d) Mass absorption cross-section, *MAC*, measured at 405 nm for the $PM_{0.1}$ (solid bars), $PM_{0.1–2.5}$ (open bars) and $PM_{2.5}$ (lined bars) fractions of BrC emitted by combustion of 50 (orange bars), 100 (blue bars), 300 (green bars) and 600 mg (red bars) of pine (c) and oak (d: purple bars) wood. (For interpretation of the references to colour in this figure legend, the reader is referred to the web version of this article.)

et al., 2020) open bars), Colorado (orange open bar (Washenfelder et al., 2022)), Alaska (blue open bar (Bali et al., 2024)) and Oregon (green open bar (Marsavin et al., 2021)). This indicates that the variation of the wood mass and type could explain, at least to some extent, the large variation of the BrC light absorption between various wildfire emissions. It should be noted that the BrC *MAC* values measured here are smaller than the *MAC* = 1.8 m^2/g measured recently for wildfire PM (Chakrabarty et al., 2023). This can be attributed to the large black carbon or EC content (~20 wt%) of that wildfire PM (Chakrabarty et al., 2023) that may enhance the measured *MAC* (Saleh et al., 2014). In contrast, the BrC measured here contains mostly organic carbon (OC) and negligible amounts of EC (<0.5 wt%; Table S1) that result in small *MAC*.

The OC and EC content of the BrC particles generated here by pine and oak wood combustion does not vary with the combusted wood mass or type (Table S1). So, the enhancement of the $MAC_{PM2.5}$ with increasing pine wood mass cannot be explained by the EC content of the BrC particles, as previous studies on biomass combustion have suggested (Saleh et al., 2014). In this regard, the impact of particle size and volatile OC (VOC) content on the BrC light absorption will be elucidated in section 3.2 and 3.3, respectively, to explain the $MAC_{PM2.5}$ variation between various combustion conditions.

3.2. Light absorption of size-fractionated BrC particles

In this section, the size-resolved light absorption of BrC particles is obtained, for the first time to the best of our knowledge. In particular, Fig. 4a shows the mass concentration of the $PM_{0.1}$, $M_{PM0.1}$, and $PM_{0.1–2.5}$, $M_{PM0.1–2.5}$, fractions of BrC emitted by combustion of 50 (orange open bar), 100 (blue dotted bar), 300 (green lined bar) and 600 mg (red filled bar) of pine wood with air. Combustion of 50 mg of pine wood (open bars) results in comparable $M_{PM0.1}$ and $M_{PM0.1–2.5}$ of about 40 mg/m^3. Increasing the fuel mass up to 600 mg, increases both $M_{PM0.1}$ and $M_{PM0.1–2.5}$. However, the fraction of large BrC particles increases with increasing fuel mass. For example, the $M_{PM0.1–2.5}$ obtained by combustion of 600 mg of pine or oak (Fig. 4b) is about two times larger than the $M_{PM0.1}$ measured at the same conditions. This is in line with the mass concentrations of particles with diameter ranging from 10–200 nm measured by SMPS (Fig. S9).

Fig. 4c shows the mass absorption cross-sections of the $PM_{0.1}$, $MAC_{PM0.1}$, and $PM_{0.1–2.5}$, $MAC_{PM0.1–2.5}$, fractions of BrC emitted by combustion of 50 (orange open bar), 100 (blue dotted bar), 300 (green lined bar) and 600 mg (red filled bar) of pine wood with air. The $MAC_{PM0.1–2.5}$ measured for BrC from combustion of 50 mg of pine wood is about five times larger than the $MAC_{PM0.1}$ measured at the same conditions. Increasing the fuel mass enhances both $MAC_{PM0.1}$ and $MAC_{PM0.1–2.5}$, but reduces the difference between them. Still, the $MAC_{PM0.1–2.5}$ measured for BrC from combustion of 600 mg of pine wood is about two times larger than the $MAC_{PM0.1}$ measured at the same conditions. So, the *MAC* enhancement with increasing pine wood mass shown in Fig. 3 can be explained by the emission of large BrC particles that absorb strongly light. The large BrC particles emitted by oak wood combustion also absorb more light compared to the smaller ones, resulting in $MAC_{PM0.1}$ = 0.25 m^2/g and $MAC_{PM0.1–2.5}$ = 0.53 m^2/g (Fig. 4d).

It should be noted that the $PM_{0.1}$ fraction of the BrC generated here by wood combustion contains more oxygenated surface groups compared to the $PM_{0.1–2.5}$ fraction (Singh et al., 2022). Such groups typically reduce the optical band gap of carbonaceous nanoparticles (Chen and Wang, 2019) and thus enhance their light absorption (Kelesidis and Pratsinis, 2019). Despite these surface effects, the $PM_{0.1–2.5}$ fraction of BrC exhibits significantly larger light absorption efficiency compared to the $PM_{0.1}$. So, the BrC *MAC* was estimated using the Mie theory for spheres with diameter, d_p = 10–2500 nm and refractive index, *RI* = 1.55–0.017i (Fig. S10: solid line) and 1.55–0.006i (broken line). Regardless of the BrC *RI*, the *MAC* of the $PM_{0.1–2.5}$ size fraction is larger than that of the $PM_{0.1}$. This indicates that the size dependence of the BrC light absorption observed here is mostly due to the Mie resonance. Reducing the imaginary part of the *RI* by 65 % decreases the BrC *MAC* up to 65 % at a given d_p. So, changes of the BrC chemical composition that alter its *RI* can explain the *MAC* variation between similar PM size fractions generated at different combustion conditions. The impact of chemical composition is corroborated, to some extent, by the PAH analysis of the BrC particles generated here. In particular, the concentration of high molecular weight (252–302 g/mol) PAHs bound on the $PM_{0.1–2.5}$ fraction is larger compared to that measured for the $PM_{0.1}$ fraction (Fig. S11). In addition, the concentration of such high molecular weight PAHs increases with increasing wood mass (Fig. S12). The enhanced light absorption of single PAHs with large molecular weight extracted from PM emissions from wood combustion (Wong et al., 2017) and wildfires (Di Lorenzo et al., 2017; Di Lorenzo and Young, 2016) has been previously reported. Here, it is shown, for the first time to the best of our knowledge, that the light absorption efficiency of BrC containing several PAHs increases with particle size. Similar *MAC* variations with particle size have been measured for flame (Dastanpour et al., 2017) and engine (Corbin et al., 2022) soot.

3.3. Impact of volatile organic carbon on BrC light absorption

In this section, the impact of low molecular weight PAHs identified here as volatile OC (VOC) on the BrC light absorption is elucidated. Such VOC coatings can be formed during atmospheric aging of PM originated from wildfires and its constituent tar balls, as revealed by recent field studies (Cheng et al., 2024). To this end, the thermal denuding temperature, T_d, is reduced from 300 to 0 °C. This increases the $PM_{2.5}$ mass concentration emitted by combustion of 600 mg of pine wood from 450 ± 49 to 1747 ± 272 mg/m^3 (Fig. 5a). The VOC to total carbon mass ratio, VOC/TC, can be determined assuming that almost all VOCs are removed at T_d = 300 °C (Saleh et al., 2018). As T_d decreases from 300 to 0 °C, VOC/TC increases from 0 up to 0.75. Reducing T_d also decreases $MAC_{PM2.5}$ from 0.6 ± 0.09 to about 0.35 ± 0.08 m^2/g (Fig. 5b). This $MAC_{PM2.5}$ reduction can be attributed to the increase of VOC that mostly scatters light, exhibits low absorption efficiency (Saleh et al., 2014) and reduces the overall particle light absorption, as shown previously by measurements (Schnaiter et al., 2006) and simulations (Kelesidis et al., 2021) of VOC-containing soot light absorption.

Similar reductions of the $MAC_{PM2.5}$ with increasing VOC content were obtained for BrC generated by combustion of 50, 100 and 300 mg using T_d = 0 °C. In particular, BrC particles emitted by combustion of 50 mg of pine wood contained 24 % less VOC compared to those obtained by combustion of 600 mg (Fig. 6a). Despite their larger VOC content, the $MAC_{PM2.5}$ of BrC emissions from combustion of 600 mg of pine wood is more than two times larger compared to that obtained using 50 mg (Fig. 6b). This indicates that the particle size largely determines the BrC light absorption even in the presence of VOC.

4. Conclusions

The dynamics of brown carbon (BrC) particles emitted during combustion of pine and oak wood and denuded from volatile organic carbon (VOC) are investigated here using an integrated incineration platform connected with a variety of real-time PM monitoring and time-integrated PM sampling instrumentation. This platform enables the detailed physicochemical characterization of BrC emissions from thermal degradation of wood at well controlled combustion conditions. So, BrC particles with controlled morphology, size distribution and light absorption were generated by varying the wood mass and type (pine and oak) to emulate the physicochemical properties of real wildfire PM emissions. That way, it is shown that increasing the wood mass from 50 to 600 mg enhances the BrC mass absorption cross-section, *MAC*. The BrC *MAC* measured at 405 nm ranges from 0.3 to 0.6 m^2/g, explaining nicely the *MAC* variation observed in the field between different wildfire

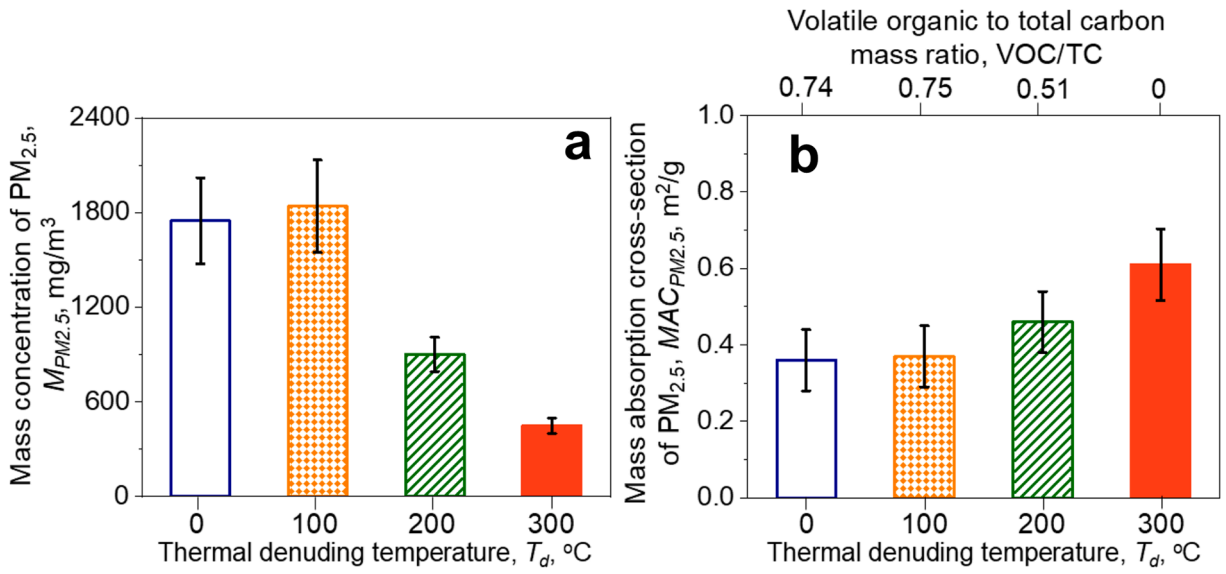

Fig. 5. Impact of volatile organics on BrC light absorption. The $M_{PM2.5}$ (a) and $MAC_{PM2.5}$ (b) measured at 405 nm for BrC emitted from combustion of 600 mg of pine wood and denuded from volatile organic carbon (VOC) at temperatures, $T_d = 0$ (purple open bars), 100 (orange dotted bars), 200 (green lined bars) and 300 °C (red filled bars). The VOC over the total carbon mass ratio, VOC/TC, is obtained based on $M_{PM2.5}$ and shown in the top axis of (b). (For interpretation of the references to colour in this figure legend, the reader is referred to the web version of this article.)

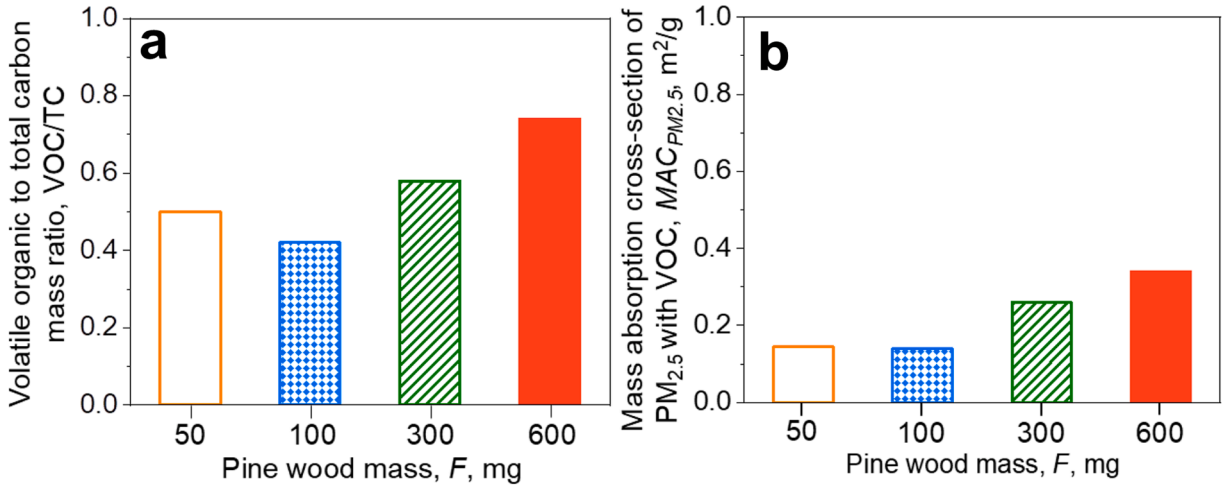

Fig. 6. Light absorption of VOC-containing BrC particles. The VOC/TC (a) and $MAC_{PM2.5}$ (b) measured at 405 nm for the $PM_{2.5}$ fraction of BrC emitted by combustion of 50 (orange open bar), 100 (blue dotted bar), 300 (green lined bar) and 600 mg (red filled bar) of pine wood using $T_d = 0$ °C. (For interpretation of the references to colour in this figure legend, the reader is referred to the web version of this article.)

PM events.

Most importantly, the light absorption of size-fractionated BrC particles was quantified, for the first time to the best of our knowledge. This reveals that the large $PM_{0.1–2.5}$ size fraction of BrC contains carcinogenic, high molecular weight PAHs and absorbs up to five times more light compared to the small size $PM_{0.1}$ fraction. So, increasing the fuel mass from 50 to 600 mg increases the $PM_{0.1–2.5}$ mass concentration and explains the enhancement of the overall BrC *MAC*. This is in line with previous field measurements showing that the concentration of high molecular weight PAHs exhibiting strong light absorption (Di Lorenzo and Young, 2016) increases with increasing particle size (Di Lorenzo et al., 2018).

The impact of VOC on the BrC light absorption is also quantified by reducing the thermal denuding temperature from 300 to 0 °C. Increasing the VOC mass concentration up to 75 wt% leads to reduction of BrC *MAC* by up to 40 %. In this regard, BrC produced by combustion of 50 mg contains 35 % less VOC compared to those emitted by combustion of 600 mg, but still absorb 50 % less light. This indicates that the particle size largely determines the BrC light absorption even in the presence of VOC.

The above findings highlight the large impact of particle size on the optical properties of BrC and suggest that measurements of size-fractionated BrC mass concentration and light absorption are essential to determine accurately the climate effects of wildfire emissions. In this regard, the size-resolved BrC *MAC* derived here can be used to obtain the absorption function and assist the monitoring of the BrC mass concentration using laser diagnostics (Kelesidis and Pratsinis, 2021). Furthermore, the *MAC* of the $PM_{0.1}$ and $PM_{0.1–2.5}$ fractions of BrC measured here can be interfaced with global climate models to quantify the contribution of wildfire PM to global warming (Kelesidis et al., 2022).

CRediT authorship contribution statement

Constantinos Moularas: Writing – original draft, Visualization,

Validation, Methodology, Investigation, Formal analysis. **Irini Tsiodra:** Writing – review & editing, Methodology, Investigation, Formal analysis. **Nikolaos Mihalopoulos:** Writing – review & editing, Resources, Methodology, Formal analysis. **Philip Demokritou:** Writing – review & editing, Resources, Funding acquisition. **Georgios A. Kelesidis:** Writing – review & editing, Supervision, Resources, Project administration, Methodology, Funding acquisition, Formal analysis, Conceptualization.

Declaration of competing interest

The authors declare that they have no known competing financial interests or personal relationships that could have appeared to influence the work reported in this paper.

Acknowledgements

This investigation was made possible partly by funding from NIH grants num. 1R01HL168899-01A1 and 1R01HL168899. Its contents are solely the responsibility of the authors and do not necessarily represent the official views of the NIH. Additionally, our research was supported by the Rutgers-NIEHS Center for Environmental Exposures and Disease (CEED) (NIH grant # P30ES005022). IT and NM acknowledge the support of Dr. Constantine Parinos from HCMR and MSc. Kalliopi Tavernaraki from ECPL for their help in PAH analysis.

Appendix A. Supplementary data

Evolution of temperature and total number concentration of brown carbon (BrC) nanoparticles as a function of time during combustion of 50 - 600 mg of pine wood; Mobility size distributions of BrC particles emitted by combustion of 50, 100, 300 and 600 mg of pine wood; Evolution of the absorption coefficient of the $PM_{2.5}$ fraction of BrC as a function of time during combustion of 50-600 mg of pine wood; Evolution of the absorption coefficients of the BrC $PM_{2.5}$ and $PM_{0.1}$ fractions as a function of time during combustion of 600 mg of pine and oak wood; Time-averaged and instantaneous mass absorption cross-section of the $PM_{0.1}$ fraction of BrC emitted by combustion of 600 mg of pine wood; Mobility size distribution of BrC emitted by combustion of 600 mg of pine or oak wood; Concentration of retene bound on the $PM_{2.5}$ fraction of BrC emitted by combustion of 50-600 mg of pine wood; Concentration of retene, carcinogenic and oxygenated PAHs bound on the $PM_{2.5}$ fraction of BrC emitted by combustion of 600 mg of oak and pine wood; Normalized mass concentration as a function of mobility diameter measured for the BrC emitted by combustion of 50-600 mg of pine wood; The mass absorption cross-section as a function of the particle diameter using a refractive index of 1.55-0.017i and 1.55-0.006i. Concentration of high molecular weight (252-302 g/mol) PAHs along with the *MAC* of the $PM_{0.1}$ and $PM_{0.1\text{-}2.5}$ fractions of BrC emitted by combustion of oak wood; Evolution of the $MAC_{PM2.5}$ as a function of the concentration of high molecular weight PAHs bound on the $PM_{2.5}$ fraction of BrC emitted by combustion of 50-600 mg of pine wood; Elemental to total carbon mass ratio of BrC emitted by combustion of various wood types and masses. Supplementary data to this article can be found online at https://doi.org/10.1016/j.envint.2025.109626.

Data availability

Data will be made available on request.

References

Abid, A.D., Heinz, N., Tolmachoff, E.D., Phares, D.J., Campbell, C.S., Wang, H., 2008. On evolution of particle size distribution functions of incipient soot in premixed ethylene-oxygen-argon flames. Combust. Flame 154, 775–788.

Bali, K., Banerji, S., Campbell, J.R., Bhakta, A.V., Chen, L.W.A., Holmes, C.D., Mao, J.Q., 2024. Measurements of brown carbon and its optical properties from boreal forest fires in Alaska summer. Atmos. Environ. 324, 120436.

Carter, T.S., Heald, C.L., Cappa, C.D., Kroll, J.H., Campos, T.L., Coe, H., Cotterell, M.I., Davies, N.W., Farmer, D.K., Fox, C., Garofalo, L.A., Hu, L., Langridge, J.M., Levin, E. J.T., Murphy, S.M., Pokhrel, R.P., Shen, Y.J., Szpek, K., Taylor, J.W., Wu, H.H., 2021. Investigating carbonaceous aerosol and its absorption properties from fires in the Western United States (WE-CAN) and Southern Africa (ORACLES and CLARIFY). J. Geophys. Res.-Atmos. 126, e2021JD034984.

Cavalli, F., Viana, M., Yttri, K.E., Genberg, J., Putaud, J.P., 2010. Toward a standardised thermal-optical protocol for measuring atmospheric organic and elemental carbon: the EUSAAR protocol. Atmos. Meas. Technol. 3, 79–89.

Chakrabarty, R.K., Moosmüller, H., Garro, M.A., Arnott, W.P., Walker, J., Susott, R.A., Babbitt, R.E., Wold, C.E., Lincoln, E.N., Hao, W.M., 2006. Emissions from the laboratory combustion of wildland fuels: particle morphology and size. J. Geophys. Res.-Atmos. 111, D07204.

Chakrabarty, R.K., Moosmüller, H., Chen, L.W.A., Lewis, K., Arnott, W.P., Mazzoleni, C., Dubey, M.K., Wold, C.E., Hao, W.M., Kreidenweis, S.M., 2010. Brown carbon in tar balls from smoldering biomass combustion. Atmos. Chem. Phys. 10, 6363–6370.

Chakrabarty, R.K., Shetty, N.J., Thind, A.S., Beeler, P., Sumlin, B.J., Zhang, C.C., Liu, P., Idrobo, J.C., Adachi, K., Wagner, N.L., Schwarz, J.P., Ahern, A., Sedlacek, A.J., Lambe, A., Daube, C., Lyu, M., Liu, C., Herndon, S., Onasch, T.B., Mishra, R., 2023. Shortwave absorption by wildfire smoke dominated by dark brown carbon. Nat. Geosci. 16, 683–688.

Chen, D.P., Wang, H., 2019. HOMO-LUMO energy splitting in polycyclic aromatic hydrocarbons and their derivatives. Proc. Combust. Inst. 37, 953–959.

Cheng, Z.Z., Shrivastava, M., Ijaz, A., Veghte, D., Vandergrift, G.W., Tseng, K.P., Lata, N. N., Kew, W., Suski, K., Weis, J., Kulkarni, G., Berg, L.K., Fast, J.D., Kovarik, L., Mazzoleni, L.R., Zelenyuk, A., China, S., 2024. Enhanced light absorption for solid-state brown carbon from wildfires due to organic and water coatings. Nat. Commun. 15, 10326.

China, S., Mazzoleni, C., Gorkowski, K., Aiken, A.C., Dubey, M.K., 2013. Morphology and mixing state of individual freshly emitted wildfire carbonaceous particles. Nat. Commun. 4, 2122.

Corbin, J.C., Czech, H., Massabò, D., de Mongeot, F.B., Jakobi, G., Liu, F., Lobo, P., Mennucci, C., Mensah, A.A., Orasche, J., Pieber, S.M., Prévôt, A.S.H., Stengel, B., Tay, L.L., Zanatta, M., Zimmermann, R., El Haddad, I., Gysel, M., 2019. Infrared-absorbing carbonaceous tar can dominate light absorption by marine-engine exhaust. npj Clim. Atmos. Sci. 2, 12.

Corbin, J.C.A., Tyler, J.J.B., Fengshan, L.A., Timothy, A.S.A., Mark, P.J.C., Prem, L.A., Greg, J.S., 2022. Size-dependent mass absorption cross-section of soot particles from various sources. Carbon 192, 438–451.

Dastanpour, R., Momenimovahed, A., Thomson, K., Olfert, J., Rogak, S., 2017. Variation of the optical properties of soot as a function of particle mass. Carbon 124, 201–211.

Demokritou, P., Lee, S.J., Ferguson, S.T., Koutrakis, P., 2004. A compact multistage (cascade) impactor for the characterization of atmospheric' aerosols. J. Aerosol Sci 35, 281–299.

Di Lorenzo, R.A., Young, C.J., 2016. Size separation method for absorption characterization in brown carbon: application to an aged biomass burning sample. Geophys. Res. Lett. 43, 458–465.

Di Lorenzo, R.A., Washenfelder, R.A., Attwood, A.R., Guo, H., Xu, L., Ng, N.L., Weber, R. J., Baumann, K., Edgerton, E., Youne, C.J., 2017. Molecular -size -separated brown carbon absorption for biomass burning aerosol at multiple field sites. Environ. Sci. Technol. 51, 3128–3137.

Di Lorenzo, R.A., Place, B.K., VandenBoer, T.C., Young, C.J., 2018. Composition of size-resolved aged boreal fire aerosols: brown carbon biomass burning tracers, and reduced nitrogen. ACS Earth Space Chem. 2, 278–285.

Garg, P., Shan, I., Lin, S.R., Gollner, M., Fernandez-Pello, C., 2023. Limiting conditions of smoldering-to-flaming transition of cellulose powder. Fire Safety J. 141, 103936.

Islam, M.M., Neyestani, S.E., Saleh, R., Grieshop, A.P., 2022. Quantifying brown carbon light absorption in real-world biofuel combustion emissions. Aerosol Sci. Technol. 56, 502–516.

Jones, M.W., Abatzoglou, J.T., Veraverbeke, S., Andela, N., Lasslop, G., Forkel, M., Smith, A.J.P., Burton, C., Betts, R.A., van der Werf, G.R., Sitch, S., Canadell, J.G., Santín, C., Kolden, C., Doerr, S.H., Le Quéré, C., 2022. Global and regional trends and drivers of fire under climate change. Rev. Geophys. 60, e2020RG000726.

Kaskaoutis, D.G., Petrinoli, K., Grivas, G., Kalkavouras, P., Tsagkaraki, M., Tavernaraki, K., Papoutsidaki, K., Stavroulas, I., Paraskevopoulou, D., Bougiatioti, A., Liakakou, E., Rashki, A., Sotiropoulou, R.E.P., Tagaris, E., Gerasopoulos, E., Mihalopoulos, N., 2024. Impact of peri-urban forest fires on air quality and aerosol optical and chemical properties: the case of the August 2021 wildfires in Athens Greece. Sci. Total Environ. 907, 168028.

Kelesidis, G.A., Pratsinis, S.E., 2019. Soot light absorption and refractive index during agglomeration and surface growth. Proc. Combust. Inst. 37, 1177–1184.

Kelesidis, G.A., Pratsinis, S.E., 2021. Determination of the volume fraction of soot accounting for its composition and morphology. Proc. Combust. Inst. 38, 1189–1196.

Kelesidis, G.A., Bruun, C.A., Pratsinis, S.E., 2021. The impact of organic carbon on soot light absorption. Carbon 172, 742–749.

Kelesidis, G.A., Neubauer, D., Fan, L.S., Lohmann, U., Pratsinis, S.E., 2022. Enhanced light absorption and radiative forcing by black carbon agglomerates. Environ. Sci. Technol. 56, 8610–8618.

Kelesidis, G.A., Nagarkar, A., Rivano, P.G., 2024. Solar steam generation enabled by carbon black: the impact of particle size and nanostructure. AIChE J. 70, e18619.

Kelesidis, G.A., Moularas, C., Parhizkar, H., Calderon, L., Tsiodra, I., Mihalopoulos, N., Kavouras, I., Korras-Carraca, M.B., Hatzianastassiou, N., Georgopoulos, P.G., Laurent, J.G.C., Demokritou, P., 2025. Radiative cooling in New York/New Jersey metropolitan areas by wildfire particulate matter emitted from the Canadian wildfires of 2023. Commun. Earth Environ. 6, 304.

Khraishah, H., Alahmad, B., Ostergard, R., AlAshqar, A., Albaghdadi, M., Vellanki, N., Chowdhury, M.M., Al-Kindi, S.G., Zanobetti, A., Gasparrini, A., Rajagopalan, S., 2022. Climate change and cardiovascular disease: implications for global health. Nat. Rev. Cardiol. 19, 798–812.

Kirchmeier-Young, M.C., Gillett, N.P., Zwiers, F.W., Cannon, A.J., Anslow, F.S., 2019. Attribution of the influence of human-induced climate change on an extreme fire season. Earths Future 7, 2–10.

Kleinman, L.I., Sedlacek, A.J., Adachi, K., Buseck, P.R., Collier, S., Dubey, M.K., Hodshire, A.L., Lewis, E., Onasch, T.B., Pierce, J.R., Shilling, J., Springston, S.R., Wang, J., Zhang, Q., Zhou, S., Yokelson, R.J., 2020. Rapid evolution of aerosol particles and their optical properties downwind of wildfires in the western US. Atmos. Chem. Phys. 20, 13319–13341.

Künzli, N., Avol, E., Wu, J., Gauderman, W.J., Rappaport, E., Millstein, J., Bennion, J., McConnell, R., Gilliland, F.D., Berhane, K., Lurmann, F., Winer, A., Peters, J.M., 2003. Health effects of the Southern California wildfires on children. Am. J. Resp. Crit. Care 174 (2006), 1221–1228.

Larson, T.V., Koenig, J.Q., 1994. Wood smoke - emissions and noncancer respiratory effects. Annu. Rev. Publ. Health 15, 133–156.

Laskin, A., Laskin, J., Nizkorodov, S.A., 2015. Chemistry of atmospheric brown carbon. Chem. Rev. 115, 4335–4382.

Laurent, J.G.C., Parhizkar, H., Calderon, L., Lizonova, D., Tsiodra, I., Mihalopoulos, N., Kavouras, I., Alam, M., Baalousha, M., Bazina, L., Kelesidis, G.A., Demokritou, P., 2024. Physicochemical characterization of the particulate matter in New Jersey/New York City Area, resulting from the Canadian Quebec Wildfires in June 2023. Environ. Sci. Technol. 58, 14753–14763.

Li, W.J., Riemer, N., Xu, L., Wang, Y.Y., Adachi, K., Shi, Z.B., Zhang, D.Z., Zheng, Z.H., Laskin, A., 2024. Microphysical properties of atmospheric soot and organic particles: measurements, modeling, and impacts. npj Clim. Atmos. Sci. 7, 65.

Liu, J.C., Mickley, L.J., Sulprizio, M.P., Dominici, F., Yue, X., Ebisu, K., Anderson, G.B., Khan, R.F.A., Bravo, M.A., Bell, M.L., 2016. Particulate air pollution from wildfires in the Western US under climate change. Clim. Change 138, 655–666.

Maetzler, C., 2002. MATLAB Functions for Mie Scattering and Absorption. University of Bern, Switzerland.

Maricq, M.M., Harris, S.J., Szente, J.J., 2003. Soot size distributions in rich premixed ethylene flames. Combust. Flame 132, 328–342.

Marsavin, A., van Gageldonk, R., Bernays, N., May, N.W., Jaffe, D.A., Fry, J.L., 2021. Optical properties of biomass burning aerosol during the 2021 Oregon fire season: comparison between wild and prescribed fires. Environ. Sci.-Atmos. 3 (2023), 608–626.

Moularas, C., Demokritou, P., Kelesidis, G.A., 2024. Light absorption dynamics of brown carbon particles during wood combustion and pyrolysis. Proc. Combust. Inst. 40, 105513.

Olson, M.R., Garcia, M.V., Robinson, M.A., Van Rooy, P., Dietenberger, M.A., Bergin, M., Schauer, J.J., 2015. Investigation of black and brown carbon multiple-wavelength-dependent light absorption from biomass and fossil fuel combustion source emissions. J. Geophys. Res.-Atmos. 120, 6682–6697.

Ramdahl, T., 1983. Retene - a molecular marker of wood combustion in ambient air. Nature 306, 580–583.

Saleh, R., 2020. From measurements to models: toward accurate representation of brown carbon in climate calculations. Curr. Pollut. Rep. 6, 90–104.

Saleh, R., Robinson, E.S., Tkacik, D.S., Ahern, A.T., Liu, S., Aiken, A.C., Sullivan, R.C., Presto, A.A., Dubey, M.K., Yokelson, R.J., Donahue, N.M., Robinson, A.L., 2014. Brownness of organics in aerosols from biomass burning linked to their black carbon content. Nat. Geosci. 7, 647–650.

Saleh, R., Cheng, Z.Z., Atwi, K., 2018. The brown-black continuum of light-absorbing combustion aerosols. Environ. Sci. Technol. Let 5, 508–513.

Samburova, V., Connolly, J., Gyawali, M., Yatavelli, R.L.N., Watts, A.C., Chakrabarty, R. K., Zielinska, B., Moosmüller, H., Khlystov, A., 2016. Polycyclic aromatic hydrocarbons in biomass-burning emissions and their contribution to light absorption and aerosol toxicity. Sci. Total Environ. 568, 391–401.

Schnaiter, M., Gimmler, M., Llamas, I., Linke, C., Jäger, C., Mutschke, H., 2006. Strong spectral dependence of light absorption by organic carbon particles formed by propane combustion. Atmos. Chem. Phys. 6, 2981–2990.

Schuller, A., Montrose, L., 2020. Influence of woodsmoke exposure on molecular mechanisms underlying Alzheimer's Disease: existing literature and gaps in our understanding. Epigen. Insights 13, 1–10.

Shen, Y.J., Pokhrel, R.P., Sullivan, A.P., Levin, E.J.T., Garofalo, L.A., Farmer, D.K., Permar, W., Hu, L., Toohey, D.W., Campos, T., Fischer, E.V., Murphy, S.M., 2024. Understanding the mechanism and importance of brown carbon bleaching across the visible spectrum in biomass burning plumes from the WE-CAN campaign. Atmos. Chem. Phys. 24, 12881–12901.

Shetty, N., Liu, P., Liang, Y.T., Sumlin, B., Daube, C., Herndon, S., Goldstein, A.H., Chakrabarty, R.K., 2023. Brown carbon absorptivity in fresh wildfire smoke: associations with volatility and chemical compound groups. Environ. Sci.-Atmos. 3, 1262–1271.

Singh, D., Tassew, D.D., Nelson, J., Chalbot, M.C.G., Kavouras, I.G., Demokritou, P., Tesfaigzi, Y., 2022. Development of an integrated platform to assess the physicochemical and toxicological properties of wood combustion particulate matter. Chem. Res. Toxicol. 35, 1541–1557.

Singh, D., Tassew, D.D., Nelson, J., Chalbot, M.C.G., Kavouras, I.G., Tesfaigzi, Y., Demokritou, P., 2023. Physicochemical and toxicological properties of wood smoke particulate matter as a function of wood species and combustion condition. J. Hazard. Mater. 441, 129874.

Sotiriou, G.A., Singh, D., Zhang, F., Wohlleben, W., Chalbot, M.C.G., Kavouras, I.G., Demokritou, P., 2015. An integrated methodology for the assessment of environmental health implications during thermal decomposition of nano-enabled products. Environ. Sci.-Nano 2, 262–272.

Tsiodra, I., Grivas, G., Tavernaraki, K., Bougiatioti, A., Apostolaki, M., Paraskevopoulou, D., Gogou, A., Parinos, C., Oikonomou, K., Tsagkaraki, M., Zarmpas, P., Nenes, A., Mihalopoulos, N., 2021. Annual exposure to polycyclic aromatic hydrocarbons in urban environments linked to wintertime wood-burning episodes. Atmos. Chem. Phys. 21, 17865–17883.

Tsiodra, I., Grivas, G., Bougiatioti, A., Tavernaraki, K., Parinos, C., Paraskevopoulou, D., Papoutsidaki, K., Tsagkaraki, M., Kozonaki, F.-A., Oikonomou, K., Nenes, A., Mihalopoulos, N., 2024. Source apportionment of particle-bound polycyclic aromatic hydrocarbons (PAHs), oxygenated PAHs (OPAHs), and their associated long-term health risks in a major European city. Sci. Total Environ. 915, 175416.

Verma, V., Polidori, A., Schauer, J.J., Shafer, M.M., Cassee, F.R., Sioutas, C., 2007. Physicochemical and toxicological profiles of particulate matter in los angeles during the october 2007 Southern California Wildfires. Environ. Sci. Technol. 43 (2009), 954–960.

Vicente, A., Alves, C., Monteiro, C., Nunes, T., Mirante, F., Cerqueira, M., Calvo, A., Pio, C., 2012. Organic speciation of aerosols from wildfires in central Portugal during summer 2009. Atmos. Environ. 57, 186–196.

Wang, Z.L., Huang, X., Xue, L., Ding, K., Lou, S.J., Zhu, A.B., Ding, A.J., 2024. Intensification of mid-latitude cyclone by aerosol-radiation interaction increases transport of canadian wildfire smoke to Northeastern US. Geophys. Res. Lett. 51, e2024GL108444.

Wardoyo, A.Y.P., Morawska, L., Ristovski, Z.D., Jamriska, M., Carr, S., Johnson, G., 2007. Size distribution of particles emitted from grass fires in the Northern Territory, Australia. Atmos. Environ. 41, 8609–8619.

Washenfelder, R.A., Azzarello, L., Ball, K., Brown, S.S., Decker, Z.C.J., Franchin, A., Fredrickson, C.D., Hayden, K., Holmes, C.D., Middlebrook, A.M., Palm, B.B., Pierce, R.B., Price, D.J., Roberts, J.M., Robinson, M.A., Thornton, J.A., Womack, C. C., Young, C.J., 2022. Complexity in the evolution, composition, and spectroscopy of brown carbon in aircraft measurements of wildfire plumes. Geophys. Res. Lett. 49, e2022GL098951.

Wentworth, G.R., Aklilu, Y.A., Landis, M.S., Hsu, Y.M., 2018. Impacts of a large boreal wildfire on ground level atmospheric concentrations of PAHs, VOCs and ozone. Atmos. Environ. 178, 19–30.

Wong, J.P.S., Nenes, A., Weber, R.J., 2017. Changes in light absorptivity of molecular weight separated brown carbon due to photolytic aging. Environ. Sci. Technol. 51, 8414–8421.

Yu, P.F., Toon, O.B., Bardeen, C.G., Zhu, Y.Q., Rosenlof, K.H., Portmann, R.W., Thornberry, T.D., Gao, R.S., Davis, S.M., Wolf, E.T., de Gouw, J., Peterson, D.A., Fromm, M.D., Robock, A., 2019. Black carbon lofts wildfire smoke high into the stratosphere to form a persistent plume. Science 365, 587–590.

Zeng, L.H., Dibb, J., Scheuer, E., Katich, J.M., Schwarz, J.P., Bourgeois, I., Peischl, J., Ryerson, T., Warneke, C., Perring, A.E., Diskin, G.S., DiGangi, J.P., Nowak, J.B., Moore, R.H., Wiggins, E.B., Pagonis, D., Guo, H.Y., Campuzano-Jost, P., Jimenez, J. L., Xu, L., Weber, R.J., 2022. Characteristics and evolution of brown carbon in western United States wildfires. Atmos. Chem. Phys. 22, 8009–8036.

Zhang, Y.Z., Forrister, H., Liu, J.M., Dibb, J., Anderson, B., Schwarz, J.P., Perring, A.E., Jimenez, J.L., Campuzano-Jost, P., Wang, Y.H., Nenes, A., Weber, R.J., 2017. Top-of-atmosphere radiative forcing affected by brown carbon in the upper troposphere. Nat. Geosci. 10, 486–489.

Zheng, G.J., Sedlacek, A.J., Aiken, A.C., Feng, Y., Watson, T.B., Raveh-Rubin, S., Uin, J., Lewis, E.R., Wang, J., 2020. Long-range transported North American wildfire aerosols observed in marine boundary layer of eastern North Atlantic. Environ. Int. 139, 105680.